

Theoretical study of H₂O–HF and H₂O–HCl: Comparison with experiment

M. M. Szcześniak^{a)} and Steve Scheiner^{b),c)}

Department of Chemistry and Biochemistry, Southern Illinois University at Carbondale, Carbondale, Illinois 62901

Y. Bouteiller

Centre de Mécanique Ondulatoire Appliquée du CNRS, Paris, France

(Received 14 June 1984; accepted 16 July 1984)

The H bonds in H₂O–HF and H₂O–HCl are studied and compared using *ab initio* molecular orbital methods and the results compared to experimental data. Basis sets used are: (i) triple valence 6-311G** and (ii) double ζ with two sets of polarization functions. Electron correlation, included via second- and third-order Møller–Plesset perturbation theory, is found to have profound effects on both systems, particularly H₂O–HCl. Both H bonds are strengthened substantially with a concomitant reduction in length. H-bond energies and geometries calculated at correlated levels are in excellent accord with available experimental information. In both systems, all levels of theory indicate the equilibrium geometry contains a pyramidal arrangement about the oxygen atom. However, the difference in energy between this structure and a C_{2v} planar arrangement is found to be small enough that consideration of probability amplitudes in the ground vibrational level leads to nearly equal likelihood of observing either geometry. Agreement between experimental vibrational frequencies in H₂O–HF and those calculated at correlated levels and involving quadratic, cubic, and quartic force constants is quite good. An explanation is offered for the increase in HX bond length which occurs at SCF and correlated levels upon H-bond formation based upon nearly linear relationships between this length on one hand and subunit dipole moment and polarizability on the other. The dispersion energy is found to be a very sensitive, almost exactly linear function of the increase of H–X bond length. This energy contributes substantially to the weakening of the HX bond upon complexation.

INTRODUCTION

H bonds of medium strength have long been a center of attention of spectroscopists and theoreticians alike. The relative simplicity of the equilibria in the gas phase was one factor in making the O–HX bond in, e.g., ether–HX and H₂O–HF,^{1–3} among the first complexes studied by gas-phase vibrational spectroscopy. It was in these systems that the band broadening and fine structure of the $\nu_0(\text{HX})$ stretching frequency were first observed. With refinement of experimental technique has come an accelerated interest in H-bonded systems. In 1975, Thomas was able to identify all of the low frequencies associated with H-bond deformations in H₂O–HF and arrived at an estimate of the potential well depth.⁴ More recently, a series of papers has been published dealing with microwave studies of the same complex. By measurement of the properties of H₂O–HF in vibrationally excited states, it has been possible to reconstruct the molecular geometry with unprecedented accuracy.^{5,6} Additionally, examination of the complex in a solid Ar matrix by Fourier-transform IR spectroscopy enabled Andrews and Johnson to provide evidence for an inversion motion.⁷ Matrix isolation techniques have also been used by Ault and Pimentel to identify the H₂O–HCl complex.⁸ More recent pulsed-nozzle Fourier-transform microwave work by Legon and Willoughby led to detection of this complex in the gas phase as well.⁹ The latter authors concluded from their measurements that the vibrationally averaged structure of H₂O–HCl

is of C_{2v} symmetry with a planar arrangement about the O atom.

Complexes of the type H₂O–HX (X = F, Cl) have provided fertile ground for theoretical studies as well. For example, several explanations have been offered for the band profile of the $\nu_s(\text{HX})$ stretching frequency. While one hypothesis draws connections with predissociation,¹⁰ recent calculations by Bouteiller and Guissani¹¹ have demonstrated the importance of anharmonic coupling between the low frequency $\nu(\text{O–F})$ and high frequency $\nu(\text{HX})$ stretching modes. SCF calculations were used by Lister and Palmieri to assign the total set of harmonic frequencies in H₂O–HF.¹² Although these assignments were quite useful, their use of a relatively small basis set resulted in an incorrect prediction of the geometry of the complex. Due to inclusion of polarization functions, more recent calculations by Bouteiller, Allavena, and Leclercq¹³ were able to successfully predict a C_s equilibrium geometry for the complex containing a pyramidal arrangement about the oxygen atom. These same investigators made an attempt to incorporate the effects of electron correlation upon the force constants within the complex but due to a somewhat limited list of configurations, found significant discrepancies between theoretical and experimental frequencies.¹⁴ Moreover, no attempt was made to study the influence of electron correlation upon the equilibrium structure of this complex or its contributions to the interaction energy. With regard to H₂O–HCl, Alagona *et al.* have provided some structural data with a medium-quality basis set at the SCF level;¹⁵ there is no information available concerning the role of electron correlation in this system.

Nevertheless, recent studies have underscored the importance of electron correlation to a true picture of H bond-

^{a)} On leave from Institute of Chemistry, University of Wrocław, Poland.

^{b)} To whom reprint requests should be addressed.

^{c)} NIH Research Career Development Awardee (1982–87).

ing. For example, the variation-perturbation treatment of the water dimer by Jeziorski and van Hemert¹⁶ demonstrated that the contribution of dispersion to the total H-bond energy is over 1/3. In their studies of the interaction between HF and CO, Benzel and Dykstra found that it is not possible to properly describe the relative stabilities of CO--HF and OC--HF without explicit account of electron correlation.¹⁷ Recent work in this laboratory has shown that dispersion plays an even more important role when second-row atoms such as Cl are involved.¹⁸

For these reasons, a major goal of the present paper is an examination of the H₂O-HF and H₂O-HCl systems which incorporates electron correlation into the procedure. The structure and properties of these complexes are studied with special emphasis placed on the effects of correlation on the interactions and shape of potential energy surfaces. As such, we perform for the first time a detailed comparison of the proton-donor properties of HF and HCl at the correlated level of theory.

While calculations that include electron correlation are generally quite time consuming and demanding of computer resources, the recent implementation of Møller-Plesset perturbation theory into molecular orbital programs by Pople *et al.* represents a significant step forward.¹⁹ It has been recently demonstrated that second-order MP theory, applied within the supermolecule framework, can yield asymptotically the dispersion energy in a well-defined manner at the uncoupled Hartree-Fock level.²⁰ Our previous results indicate great usefulness of the MP2 method in the treatment of selected H bonds.²¹ However, this procedure has not been sufficiently tested at this point to assure that truncation of the perturbation expansion after the second-order term can produce data which are comparable with experiment. A second aim of this work is therefore a stringent test of the MP2 method; recently obtained high-quality experimental results^{5,6,9} for H₂O-HF and H₂O-HCl provide an exceptional opportunity for careful comparison with theoretical calculations.

METHODS

Electron correlation was included via Møller-Plesset perturbation theory to second (MP2) and third (MP3) orders, as implemented in the GAUSSIAN-80 package of computer codes.²² Previous experience has shown that MP3 treatment of H-bonded systems with the 6-311G** basis set can closely reproduce the first term, C_6R^{-6} , of the multipole-expanded dispersion energy based on the nonempirical Unsöld approximation²¹ and we accordingly perform some of our calculations with this basis set, denoted herein as A. On the other hand, a more accurate treatment of dispersion at the MP2 level requires at least two sets of polarization functions. Our doubly polarized basis set B was constructed as follows. The double-zeta [432/21] basis set, used previously by Jeziorski and van Hemert¹⁶ and by us,²¹ was applied to the H₂O molecule; the *d*-orbital exponents used were 0.4 and 1.5. For HF, the 6-31G basis set was augmented by two sets of *d* functions on F (exponents 0.25 and 1.0) and two sets of *p* functions on H (0.15 and 0.75). The latter exponents were chosen according to the suggestion of van Duijneveldt²³ who

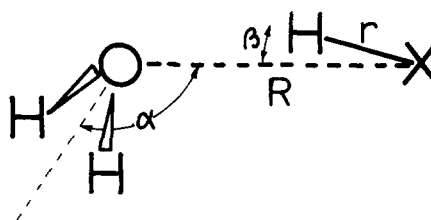


FIG. 1. C_s geometrical parameters for H₂O-HX (X = F, Cl). α measures the angle between the O-X axis and the OH₂ bisector.

obtained good dipole polarizabilities using them. The B basis set for Cl consists of the 6-6-31G set, supplemented by *d* functions with exponents 0.25 and 0.75, taken from van Duijneveldt.²³

RESULTS

Structure and vibrations of H₂O-HF

The structural parameters of the H₂O-HX complexes are illustrated in Fig. 1 where R is defined as the distance between O and X atoms. β measures the deviation of the H atom from the O-X axis and α is the angle between this axis and the HOH bisector. Geometry optimizations of the H₂O-HF complex were carried out with basis set A and the results are presented in Table I. In these optimizations, the internal geometry of the H₂O molecule was held fixed in its experimentally determined structure; $r(\text{OH}) = 0.957 \text{ \AA}$ and $\theta(\text{HOH}) = 104.5^\circ$. Gradient procedures were used to optimize the structure at the SCF level and stepwise procedures at the correlated levels.

We may see from the results at SCF as well as at correlated levels, that the optimized structure is of C_s symmetry, with a pyramidal oxygen atom, in agreement with experimental findings²⁴ as well as previous calculations¹³ with polarized basis sets. Slight nonlinearities of the H bond are noted in that the equilibrium values of β are somewhat greater than zero. The intermolecular separations R are smaller at correlated levels than the SCF value, with the MP2 distance slightly smaller than MP3. A similar pattern is noted for α , the pyramidalization angle of oxygen. Table I indicates that the MP3 procedure, in conjunction with basis set A, is capable of closely reproducing experimental data, listed in the last column of the table. The effects of correlation upon the SCF structure are as follows. The intermolecular distance is decreased, concomitant with an increase in the internal HF bond length and a trend toward a more perpendicular arrangement of the H₂O molecule; i.e., reduction of α . This tendency toward smaller α may be explained on elec-

TABLE I. Values of geometrical parameters (see Fig. 1) of H₂O...HF calculated with basis set A.

	SCF	MP2	MP3	Experiment ^a
$R, \text{ \AA}$	2.702	2.639	2.649	2.664
$r, \text{ \AA}$	0.907	0.923	0.921	...
$\alpha, \text{ deg}$	140.3	128.8	132.7	134
$\beta, \text{ deg}$	3.1	4.5	2.5	...

^a From Ref. 24.

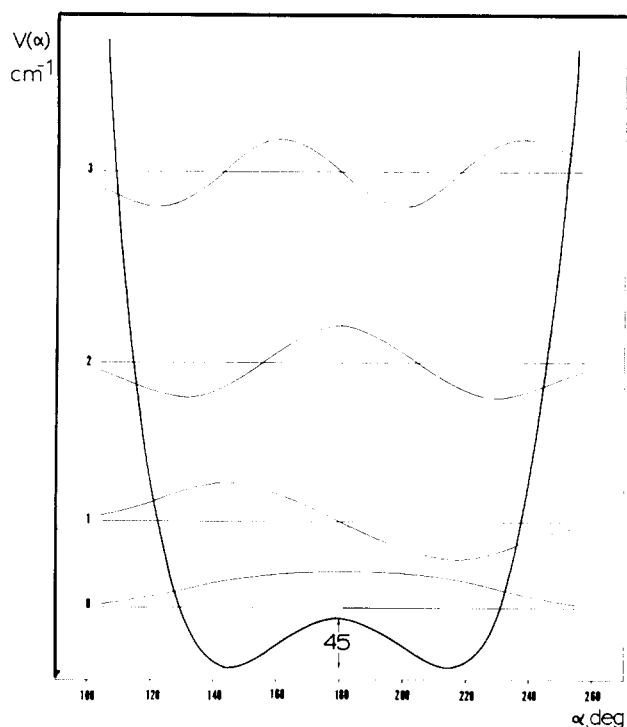


FIG. 2. Total SCF/A energy of H₂O–HF as a function of α . Vibrational energy levels and associated wave functions are superposed.

trostatic grounds as follows. The attraction between the dipole moments of the two molecules would favor large values of α which more closely align the moments. Correlation effects have been demonstrated previously to reduce the dipole moment of water²⁵ and would thereby diminish the pull toward high α . In this same regard, it is likely that the earlier predictions of a planar O atom by unpolarized basis sets were due to their well known exaggeration of dipole moments.

The exact degree of pyramidalization of the oxygen atom is a product of a delicate balance between a number of opposing forces. Whereas dipole-dipole interactions favor the planar arrangement, a more perpendicular configuration arises from consideration of dipole-quadrupole terms.²⁶ In addition to electrostatic effects, other forces such as exchange, polarization, charge transfer, and dispersion each have a different angular dependence. The net result is a very small energy difference between the planar and pyramidal geometries. The potential energy curve for the bending of the water molecule at the SCF level is shown in Fig. 2. This curve was computed by holding fixed the geometry of the complex at the values indicated in Table I and varying α between 105° and 255° (β was set equal to 0° to assure symmetry of the curve). The symmetric potential contains two equivalent minima, corresponding to a pyramidal oxygen, separated by a configuration ($\alpha = 180^\circ$) containing a planar O atom. Figures 3 and 4 illustrate the analogous potentials computed at the MP2 and MP3 levels (also using the SCF geometrical parameters and the A basis set). Superimposed on each potential energy curve is a series of vibrational levels obtained from the potential by the method of Somorjai and Hornig for evaluation of anharmonic frequencies in a double minimum potential.²⁷

The calculated results are summarized in Table II

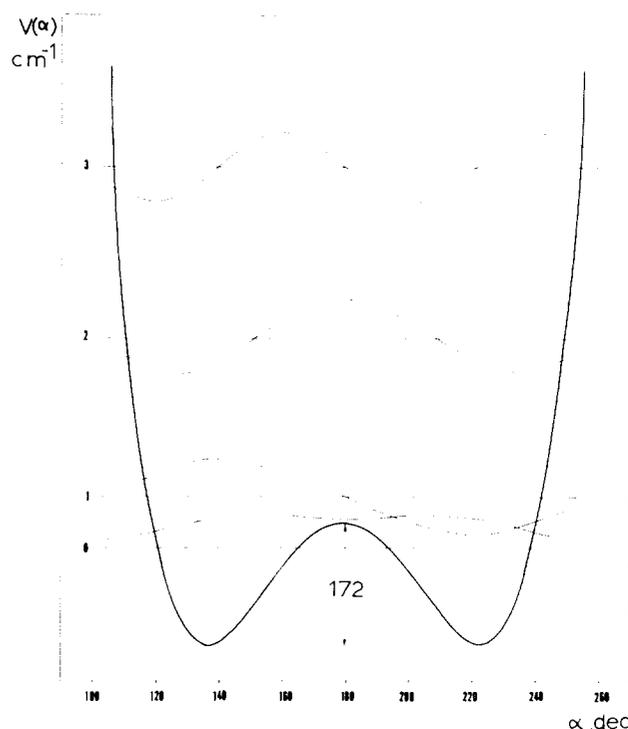


FIG. 3. MP2/A potential for inversion of water in H₂O–HF.

where they are compared with experimental data.²⁴ The first row contains the energy barrier to the inversion between the two symmetric minima. It is clear that, whereas the SCF barrier is quite small, the values obtained at correlated levels are several times larger and in much better accord with the experimental estimate. Also included in Table II are the energy differences between the ground vibrational level and the first two excited levels. The SCF treatment greatly overesti-

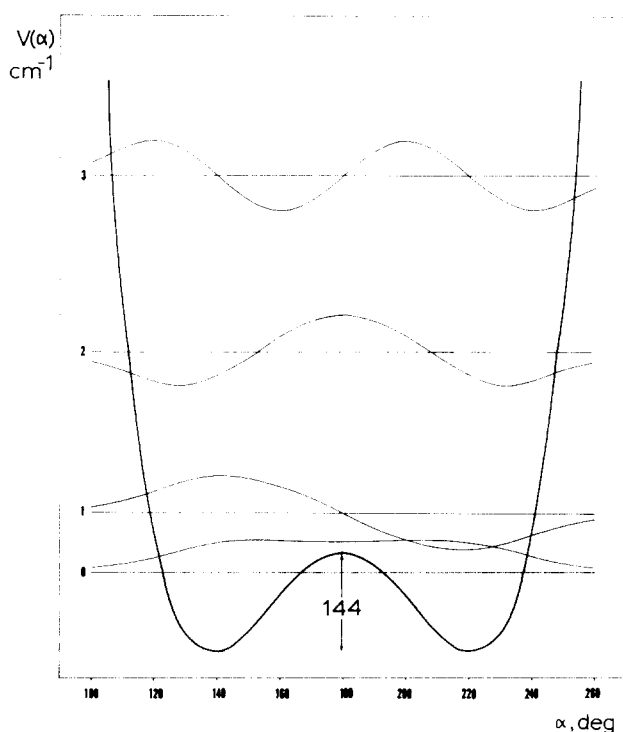


FIG. 4. MP3/A energy of H₂O–HF as a function of α .

TABLE II. Height of barrier and vibrational energy level differences^a in H₂O–HF for the low-frequency in-plane bending mode corresponding to water inversion.

	SCF	MP2	MP3	Experiment ^b
E^\ddagger	45	172	144	126
$\nu = 1 \leftarrow 0$	134	85	96	64 ± 10
$\nu = 2 \leftarrow 0$	257	251	255	267 ± 35

^a All entries in cm⁻¹; calculated with basis set A.^b Reference 24.

mates the spacing between the ground and first excited level; MP values are again closer to the experimental information. It is clear from the last row in Table II that the energy difference between the ground and second excited state is rather insensitive to inclusion of electron correlation. The overall conclusion from this table is that consideration of the effects of correlation greatly improves the agreement between calculated and experimental data and that MP3 treatment with basis set A leads to quite reasonable data.

A fundamentally important point concerns the correspondence between the theoretical and experimental equilibrium geometries. By definition, the equilibrium structure refers to the absolute minimum in the potential energy surface of the molecule. Whereas it is possible in principle to locate this minimum by theoretical methods, the ground state vibrational motions may sometimes obscure the experimental elucidation of the minimum. In the SCF potential of Fig. 2, the ground vibrational level lies slightly higher in energy than the planar structure separating the two minima. The vibrational wave function, superposed on this energy level has its maximum amplitude for the planar structure with $\alpha = 180^\circ$, leading to a likelihood of observing this structure despite the fact that it is not the minimum of the potential. However, the flatness of the function indicates that the probability of observing pyramidal arrangements with α deviating from 180° by up to perhaps 30° is not much less than the planar geometry. The situation is somewhat different in the MP potentials depicted in Figs. 3 and 4 where the ground vibrational level lies below the barrier. Nonetheless, the wave functions are quite similar to the SCF function (despite the presence of a very shallow minimum at $\alpha = 180^\circ$) and the geometry is not strongly localized in the pyramidal configuration. In a dynamical sense, then, the SCF situation in Fig. 2 where the lowest vibrational level lies above the symmetric structure is virtually indistinguishable from the MP cases depicted in Figs. 3 and 4 where the opposite is true. We conclude that accommodation of a ground vibrational level below an energy barrier is not sufficient to guarantee a dynamic distinction from a case where the level cannot be so placed; disparities arise only as the barrier height is further increased.

While the MP3 data compare fairly well with the experimental information in Table II, there remains some difference. Part of this discrepancy is probably due to limitations of basis set and finite perturbation expansion. More important, perhaps, is the treatment of the bending potential in isolation from the other geometrical parameters. The bending of the water molecule is quite likely coupled to other

TABLE III. Quadratic, cubic, and quartic force constants for H₂O–HF (in mdyn/Åⁿ), calculated with basis set A.

F	SCF	MP2
r^2	9.967	8.497
rR	0.123	1.128
R^2	0.228	0.335
r^3	-78.15	-68.96
r^2R	2.433	2.264
rR^2	0.317	0.995
R^3	-1.013	-1.789
r^4	438.5	488.5
r^3R	25.14	2.448
r^2R^2	-24.94	-10.01
rR^3	-1.783	-9.354
R^4	6.600	8.194

motions such as an intermolecular stretch or bending involving the H-bonding proton of HF. Treatment of the mode as a pure HOH bend was adopted here to match as closely as possible the one-dimensional model used by Kisiel, Legon, and Millen in their reconstruction of the potential.⁶

The preceding discussions have included a description of the anharmonicity of the bending of the water molecule relative to the HF subunit. The anomalous behavior of the band profile of the ν_s (HF) stretching frequency has also been explained on the basis of anharmonic effects, specifically as a coupling between the $\nu(\text{O--F})$ and $\nu(\text{FH})$ stretching modes.¹¹ In order to calculate anharmonic stretching frequencies, the energy was calculated for a two-dimensional grid of points in the vicinity of the equilibrium geometry. These energies $E(r, R)$ were evaluated at both the SCF and MP2 levels in order to ascertain the effects of electron correlation upon the results. Except for $r(\text{HF})$ and $R(\text{O--F})$, all geometrical parameters were held fixed in the values optimized previously with basis set A. Table III contains the quadratic, cubic, and quartic force constants evaluated by numerical analysis of the computed potential energy surfaces. Comparison of the SCF and MP2 constants reveals the effects of electron correlation upon these constants. For the most part, these changes are qualitatively similar to the trends found previously by Bouteiller *et al.*¹⁴ There are, however, some large quantitative and even qualitative disparities in the results which have some bearing on the next point to be discussed concerning vibrational frequencies.

The procedure described in Ref. 28 for extracting the vibrational frequencies from all force constants up through fourth order was applied to the data in Table III and the

TABLE IV. Stretching frequencies in H₂O–HF (in cm⁻¹).

	This work		Ref. 14				
	A		6-31G*				
	SCF	MP2	SCF	SCF	SD	SDQ	Expt
$\nu(\text{FH})$	4013	3764	3824	4051	4031	3946	3608 ^a
$\nu(\text{O--F})$	204	236	198	222	242	242	198 ^b

^a Reference 4.^b Reference 29.

TABLE V. Calculated geometries and interaction energies.

	H ₂ O–HF				H ₂ O–HCl	
	A		B		B	
	SCF	MP2	SCF	MP2	SCF	MP2
<i>R</i> (OX), Å	2.70	2.65 ^a	2.71	2.65	3.37	3.19
<i>r</i> , Å	0.907	0.921 ^a	0.912	0.939	1.277	1.290
Δr , Å	0.011	0.012 ^a	0.012	0.017	0.009	0.015
ΔE^{SCF} , kcal/mol	– 9.38	– 9.19	– 7.76	– 7.06	– 4.16	– 3.83
ΔE^{MP2} , kcal/mol	– 10.51	– 11.03 ^b	– 9.15	– 9.64	– 6.22	– 6.59

^a Geometry optimized with MP3.

^b MP3 value is – 10.49.

results are presented in Table IV. It may be seen that the application of MP2 to the A basis set improves the agreement of $\nu(\text{FH})$ with the experimental value markedly. In fact, the MP2/A result is the best calculated value to date, much superior to the previous estimates with the 6-31G* basis set. In the case of the lower frequency vibration $\nu(\text{O}--\text{F})$, all theoretical data lead to overestimates of the experimental data, probably associated with the exaggerations of the strength of the H bond. To test the effects of further extension of the basis set, calculations were carried out with basis set C which contains the same atomic orbitals as does B for the H₂O subunit but the description of HF is improved by use of a [742/31] basis set suggested previously by Lischka.³⁰ As may be seen in the appropriate column of Table IV, the larger basis set decreases both stretching frequencies. Using the comparison between MP2 and SCF/A results as a guide, it is expected that inclusion of correlation to the SCF/C data would lead to excellent reproduction of experimental frequencies.

H-bond energies

Although the MP3 treatment with the singly polarized A basis set has been seen above to adequately reproduce experimental information concerning the equilibrium geometries and vibrational frequencies, this approach is somewhat less satisfactory for study of the energy of interaction between the subsystems. Table V contains geometries optimized with each basis set at both SCF and correlated levels. The fourth row lists the interaction energies computed at the SCF level for each geometry; analogous MP2 energies are contained in the last row.

Since the SCF and MP geometries are significantly different, there is some ambiguity in assigning a value to the increase in H-bond energy associated with correlation. Let us consider, for example, basis set A calculations of the H₂O–HF system. As may be seen in the first column of Table V, MP2 treatment of the geometry optimized at the SCF level raises the interaction energy from – 9.38 kcal/mol to – 10.51, an increase of – 1.13. However, the SCF geometry does not correspond to the bottom of the MP potential and consequently the above procedure does not indicate the full magnitude of the correlation effect. Optimization of the geometry at the MP level further increases the interaction energy to – 11.03 kcal/mol.

From a computational point of view, the full effect of

correlation is obtained by comparison of complete correlation treatment ($\Delta E^{\text{MP}}//\text{MP}$ geometry) with the SCF results ($\Delta E^{\text{SCF}}//\text{SCF}$ geometry). On the other hand, for the purpose of studying radial and angular dependence of the dispersion component, ΔE^{MP2} and ΔE^{SCF} must refer to the same geometry. For this reason, the dispersion contribution to the H-bond energy will be referred to below as the difference between ΔE^{MP2} and ΔE^{SCF} , both evaluated with the MP geometry. For the systems being examined here, the MP2 interaction energies computed with the SCF and MP geometries differ by about 0.5 kcal/mol. Thus, one would underestimate the complexation energies by this amount if MP2 were simply applied to a geometry optimized at the SCF level. Coupling this fact with the difference in SCF interaction energies between the two geometries would lead to a more severe underestimate of the contribution of dispersion to the stability of each complex. For example, using SCF geometries for H₂O–HF with basis set B, correlation contributes 1.39 kcal/mol (9.15 – 7.76), or 15% to the total interaction energy, whereas the corresponding contribution with MP2 geometries is 2.58 kcal/mol or 27%.

We expect our MP2/B estimate of the interaction energy in H₂O–HF to be fairly reliable. In addition to its good representation of electrostatic attraction (see Table VI for calculated values of subsystem dipole moments) and adequate framework for correlation and induction, the superposition error is rather small. Evaluation of this error by the counterpoise procedure yields a value of 0.7 kcal/mol at the SCF level. Subtraction of this quantity from the MP2/B interaction energy in Table V provides our best theoretical estimate of – 8.9 kcal/mol. Cancellation is expected between small additional corrections that might be added. For example, the absence of *f* orbitals, needed for good representation of quadrupole polarizabilities (and R^{-10} term of dispersion energy) will probably lead to a slight underesti-

TABLE VI. SCF and experimental dipole moments (*D*).

	A	B	Experiment
H ₂ O	2.17	2.06	1.85 ^a
HF	2.00	1.86	1.83 ^b
HCl	...	1.18	1.09 ^c

^a Reference 31.

^b Reference 32.

^c Reference 33.

mate. On the other hand, the reverse trend may be expected from truncation of the MP expansion at second order. (Although no calculations have been performed to date which incorporate the full fourth order of perturbation theory for H bonds, polarizability calculations suggest that considerable cancellation occurs between the third and *full* fourth orders.³⁴)

The enthalpy of formation of the H₂O–HF complex has been measured in the gas phase⁴ and is equal to -6.2 ± 1 kcal/mol at 298 K. Before comparison of our theoretical estimate of the electronic energy with this experimental quantity, it is first necessary to make adjustments for changes in translational, rotational, and vibrational energy, as well as addition of a ΔPV term. All the corrections, exclusive of the vibrational term, are straightforward to calculate from standard thermodynamical formulas and amount to -2.4 kcal/mol. Evaluation of the vibrational correction requires knowledge of all the frequencies in both the complex and the isolated subsystems. Much of this information is provided by Lister and Palmieri¹² who provide experimental data where available and supplement the remaining frequencies with calculated quantities. Using the frequencies supplied by these authors, we arrive at a vibrational energy difference between the complex and subsystems of 4.4 kcal/mol at 298 K. Combining all the adjustments together with our computed ΔE° of -8.9 kcal/mol leads to a value of -6.9 kcal/mol for ΔH_{298}° which falls well within the range of experimental uncertainty.

Comparison of H₂O–HCl with H₂O–HF

The complex of H₂O with HCl was studied using the doubly polarized B basis set only. Like H₂O–HF, the optimized geometry of this complex belongs to the C_s point group. The bending potential for the OH₂ molecule at both the SCF and MP levels is illustrated in Fig. 5. As in the previous case of H₂O–HF, correlation substantially raises the barrier for this motion and shifts the equilibrium value of α away from the planar configuration. The O–H–Cl bridge is slightly nonlinear with β equal to 2.8° at the SCF level and 0.9° with MP2. The optimized values of R (O–Cl) and r (HCl) are contained in Table V where it may be seen that the MP2/B H–bond length of 3.19 Å is rather close to the experimental estimate of 3.21 Å.⁹

Although experimental data⁹ indicate a planar (C_{2v}) geometry for the H₂O–HCl complex, the large amplitude motion of the H₂O unit and associated vibrational averaging makes it difficult to distinguish between this geometry and the C_s pyramidal arrangement. As may be seen in Fig. 5, the calculated barrier for inversion between the two equivalent C_s geometries is 116 cm⁻¹ at the MP2/B level. Comparison with the data for H₂O–HF in Figs. 2–4 makes it clear that as in the previous case, the ground vibrational energy will occur close to the top of the barrier and consequently the wave function will have little difference in probability amplitude between the planar and pyramidal geometries. The observation of a C_{2v} structure would therefore be consistent with a double well potential with low barrier as predicted by the calculations.

In their attempt to reconstruct the molecular geometry of H₂O–HCl from measured rotational constants, Legon

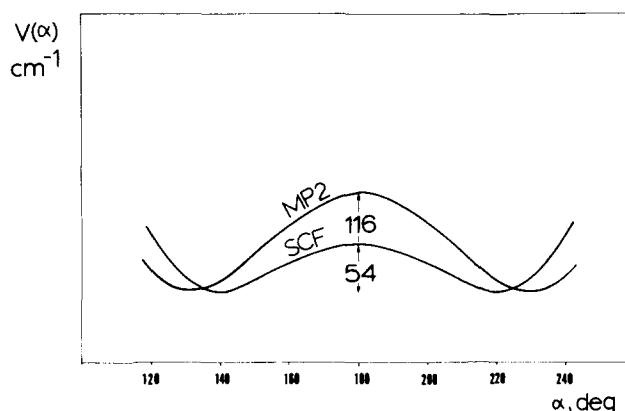


FIG. 5. Water inversion potential for H₂O–HCl calculated with basis set B.

and Willoughby⁹ suggested that the internal HOH angle increases by 4° upon complexation. We checked this hypothesis theoretically at the MP2 level. It was found that while some increase in this angle was observed, the magnitude of this increase was only 0.5°.

The energetic data in Table V indicate that the H-bond in H₂O–HCl is somewhat weaker than in H₂O–HF. Comparing the results within the framework of the B basis set, the O–H–F bond is stronger than O–H–Cl by 3.6 kcal/mol at the SCF level and 3.0 at MP2. Another important distinction concerns the contribution of correlation to the stability of each bond. This contribution is somewhat higher in H₂O–HCl (2.4 vs 1.9 kcal/mol). If one is considering the relative contributions of correlation, this difference is even more striking. Whereas correlation amounts to 20% of the total interaction energy in H₂O–HF, this term increases to 37% in H₂O–HCl. Using the previous definition of dispersion as the difference between ΔE^{MP2} and ΔE^{SCF} with MP geometry, the percentage contribution of dispersion is 27% in H₂O–HF and 42% in H₂O–HCl. Another indication of the relative importance of correlation in the two systems comes from a comparison of equilibrium H-bond lengths. The distance between oxygen and fluorine is diminished by 0.06 Å by correlation while the shortening of the O–Cl separation is three times that amount.

It is well known that the length of the HX bond is increased upon formation of a H bond such as H₂O–HX. The magnitude of this bond stretch is provided in the third row of Table V as Δr . For H₂O–HF this lengthening is 0.012 Å at the SCF level; the corresponding value for H₂O–HCl is 0.009 Å. Correlation increases this stretch to 0.017 Å in the former system and to 0.015 Å in the latter. Concomitant with these bond lengthenings is a reduction in the associated F_{rr} force constant. At the SCF level, this constant is reduced by 1.5 mdyne/Å following complexation; the analogous value at the MP2 level is 2.0. Based on previous experience, the correlation-induced bond stretches are probably somewhat exaggerated. Future calculations including higher-order perturbation effects would be quite useful in order to determine the true magnitude of the effect of correlation upon the bond length.

A very interesting and useful relationship is observed if one plots the contribution of electron correlation to the total interaction energy against the r (HX) bond length in the hy-

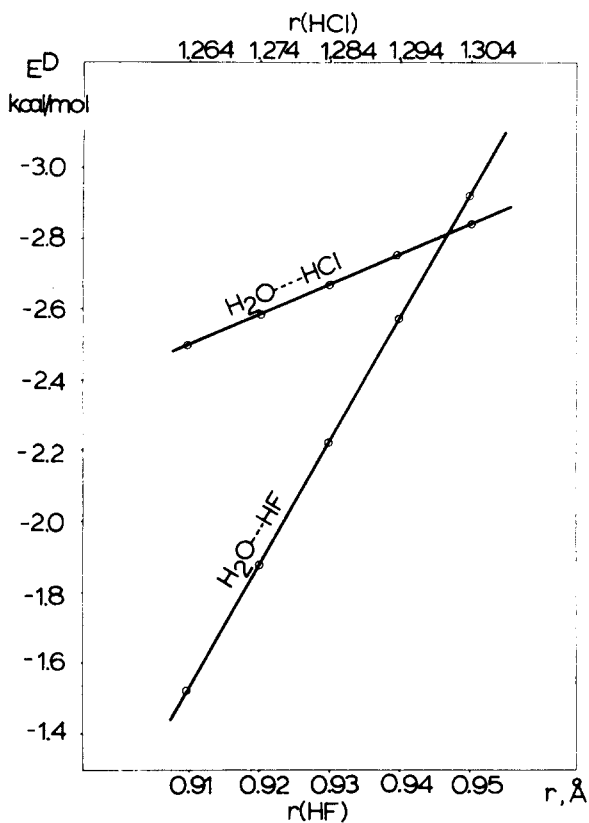


FIG. 6. Dispersion energy E^D shown as a function of $r(\text{HX})$. The lower scale is for H₂O–HF and the upper for H₂O–HCl.

drogen halide. The data in Fig. 6 indicate a very nearly exact linear relation between these two quantities. That is, as the proton is shifted away from the halogen atom, the attractive dispersion between the two molecules is increased accordingly. The slope of the curve for H₂O–HF is dramatically steeper than for H₂O–HCl: the values of dE^D/dr are -34.6 and -8.3 kcal/mol Å, respectively. Treating the dispersion energy in terms of interactions between the polarizabilities of the individual molecules, the linear relationship implies that the polarizability of HX, like its dipole moment, increases linearly with bond length. This rather dramatic increase of dispersion stabilization occurs at the expense of the energy required to stretch the H–X bond.

Early theories of H bonding attempted to explain the observed lengthening of the HX bond upon complexation on the basis of charge transfer to a vacant antibonding orbital of the proton donor.^{35–37} The results described here indicate that the bond stretch may be ascribed instead to a number of other effects. The increased dipole moment arising from the bond stretch would be expected to magnify the stabilizing electrostatic forces. Attractive induction forces would also be increased as a result of the greater polarizability (and dipole moment) of the HX molecule. These stabilizing considerations explain the amount of Δr accounted for at the SCF level and they basically agree with the earlier concepts. What is new, is our observation that dispersion forces play an important additional role in the process of lengthening of the HX bond.

We may summarize the differences between the H bonds in H₂O–HF and H₂O–HCl as follows. HF has a

greater dipole moment than does HCl and H-bonds involving HF will hence contain a greater amount of electrostatic stabilization. The smaller contribution of dispersion to the H bond in H₂O–HF is a result of the lower polarizability of the HF molecule. On the other hand, the high sensitivity of the polarizability of HF to the bond length allows the latter deficiency to be made up by small stretches of the bond upon complexation. Calculated Δr for H₂O–HF is slightly larger than that for H₂O–HCl, which agrees with the experimentally observed larger low-frequency shifts of $\nu_s(\text{HX})$ in H bonded complexes involving HF.³⁸

ACKNOWLEDGMENTS

Financial support was provided by grants to S. S. from NIH (GM29391 and AM01059) and from the Research Corporation. Allocations of computer time from SIU are acknowledged.

- ¹J. E. Bertie and D. J. Millen, *J. Chem. Soc.* **1965**, 497, 514.
- ²J. Arnold and D. J. Millen, *J. Chem. Soc.* **1965**, 503.
- ³R. K. Thomas, *Proc. R. Soc. London Ser. A* **322**, 137 (1971).
- ⁴R. K. Thomas, *Proc. R. Soc. London Ser. A* **344**, 579 (1975).
- ⁵Z. Kisiel, A. C. Legon, and D. J. Millen, *J. Chem. Phys.* **78**, 2910 (1983).
- ⁶Z. Kisiel, A. C. Legon, and D. J. Millen, *Proc. R. Soc. London Ser. A* **381**, 419 (1982).
- ⁷L. Andrews and G. L. Johnson, *J. Chem. Phys.* **79**, 3670 (1983).
- ⁸B. S. Ault and G. C. Pimentel, *J. Phys. Chem.* **77**, 57 (1973).
- ⁹A. C. Legon and L. C. Willoughby, *Chem. Phys. Lett.* **95**, 449 (1983).
- ¹⁰M.-M. Audibert and E. Palange, *Chem. Phys. Lett.* **101**, 407 (1983).
- ¹¹Y. Bouteiller and Y. Guissani, *Chem. Phys. Lett.* **69**, 280 (1980).
- ¹²D. G. Lister and P. Palmieri, *J. Mol. Struct.* **39**, 296 (1977).
- ¹³Y. Bouteiller, M. Allavena, and J. M. Leclercq, *Chem. Phys. Lett.* **69**, 521 (1980).
- ¹⁴Y. Bouteiller, M. Allavena, and J. M. Leclercq, *Chem. Phys. Lett.* **84**, 361 (1981).
- ¹⁵G. Alagona, E. Scrocco, and J. Tomasi, *Theor. Chim. Acta* **47**, 133 (1978).
- ¹⁶B. Jeziorski and M. van Hemert, *Mol. Phys.* **31**, 713 (1976).
- ¹⁷M. A. Benzel and C. E. Dykstra, *Chem. Phys.* **80**, 273 (1983).
- ¹⁸Z. Latajka and S. Scheiner, *J. Chem. Phys.* **81**, 2713 (1984); *ibid.* (in press); Z. Latajka and S. Scheiner, *Chem. Phys.* (submitted).
- ¹⁹J. A. Pople, J. S. Binkley, and R. Seeger, *Int. J. Quantum Chem. Symp.* **10**, 1 (1976).
- ²⁰A. Szabo and N. S. Ostlund, *J. Chem. Phys.* **67**, 4351 (1977).
- ²¹M. M. Szczesniak and S. Scheiner, *J. Chem. Phys.* **80**, 1535 (1984).
- ²²J. S. Binkley, R. A. Whiteside, R. Krishnan, R. Seeger, D. J. DeFrees, H. B. Schlegel, S. Topiol, L. R. Kahn, and J. A. Pople, *GAUSSIAN-80, Quantum Chem. Program Exchange* 406 (1981).
- ²³J. G. C. M. van Duijneveldt-van de Rijdt and F. B. van Duijneveldt, *J. Mol. Struct.* **89**, 185 (1982).
- ²⁴A. C. Legon and D. J. Millen, *Faraday Discuss. Chem. Soc.* **73**, 71 (1982).
- ²⁵G. H. F. Diercksen and A. J. Sadlej, *J. Chem. Phys.* **75**, 1253 (1981).
- ²⁶This is only a qualitative picture; quantitative analysis would require consideration of possible lack of convergence of the multipole expansion of electrostatic energy due to penetration effects.
- ²⁷R. L. Somorjai and D. F. Hornig, *J. Chem. Phys.* **36**, 1980 (1962).
- ²⁸Y. Bouteiller, M. Allavena, and J. M. Leclercq, *J. Chem. Phys.* **73**, 71 (1982).
- ²⁹J. W. Bevan, A. C. Legon, D. J. Millen, and S. C. Rogers, *J. Chem. Soc. Chem. Commun.* **1975**, 341.
- ³⁰H. Lischka, *J. Am. Chem. Soc.* **96**, 4761 (1974).
- ³¹J. A. Clough, Y. Beers, G. P. Klein, and L. S. Rothman, *J. Chem. Phys.* **59**, 2254 (1973).
- ³²J. S. Muentzer and W. Klemperer, *J. Chem. Phys.* **52**, 6033 (1970).
- ³³F. H. de Leeuw and A. Dymanus, *J. Mol. Spectrosc.* **48**, 427 (1973).
- ³⁴G. H. F. Diercksen, V. Kellö, and A. J. Sadlej, *Chem. Phys. Lett.* **95**, 226 (1983).
- ³⁵R. S. Mulliken, *J. Chim. Phys.* **61**, 20 (1964).
- ³⁶K. Szczesniak and A. Tramer, *J. Phys. Chem.* **71**, 3035 (1967).
- ³⁷H. Ratajczak, *J. Phys. Chem.* **76**, 3000, 3091 (1972).
- ³⁸D. J. Millen and O. Schrems, *Chem. Phys. Lett.* **101**, 320 (1983).